J Mater Sci: Mater Med (2008) 19:233–238
DOI 10.1007/s10856-006-0109-7

Preparation and characterization of selenium incorporated anodic conversion coatings on titanium surfaces for biomedical applications

J. P. Schreckenbach · H.-L. Graf

Received: 29 May 2006 / Accepted: 11 December 2006 / Published online: 28 June 2007

Abstract An anodic spark deposition process was used for preparation of inorganic, glass-ceramic like conversion coatings. The microstructure of the layers was characterized by surface and solid state techniques such as scanning electron microscopy, electron probe microanalysis and Raman spectroscopy. The porous coatings, typically up to 8 μm thick, consist mainly of titanium oxides and amounts of incorporated electrolyte constituents like Se, Ca or P. Beside nano crystalline anatase phases, a mostly amorphous structure is proposed in which network-forming [PO_4] tetrahedras and [TiO_6] octahedras in various degrees of condensation are connected. A drastic modification of the film structure was observed when selenium was incorporated into the glassy oxide structure of the coating. In these cases no nano crystalline phases of titanium oxides or other chemical compounds were detected. First cell culture investigations show a significant improvement of the biological properties. Cell proliferation and TGF-beta-expression of these coatings in comparison with commercial pure titanium (CPT) with native titanium oxide films were examined.

J. P. Schreckenbach (✉)
Department of Chemistry, Technical University of Chemnitz, 09107 Chemnitz, Germany
e-mail: joachim.schreckenbach@Chemie.TU-Chemnitz.de

H.-L. Graf
Department of Oral- Maxillo- and Facial Plastic Surgery, University of Leipzig, 04103 Leipzig, Germany

Introduction

Materials processing and surface modification by electrochemical methods play an important role among the techniques for fabrication of new coating materials and microstructures. Anodic spark deposition (ASD) is an advanced plasmachemical-electrochemical method of forming ceramic like surfaces on anodic metal substrates of valve metals. There is a normal anodizing or oxidation process on the anodic metal surface, which occurs before ASD and is called "pre-sparking anodization." This is the precursor state for anodic spark deposition. Further increase in the potential causes dielectric breakdowns, accompanied by visible micro plasma sparking at the anode surface and the formation of novel glass ceramic films during this process [1–6]. In the literature different designations for this treatment and the corresponding coatings are used. Beside ASD, dielectric breakdown process, micro arc oxidation, plasma electrolytic oxidation (PEO), Ticer, TiUnite, anodic plasma-chemical process (APC) are found [5–11]. This promising surface treatment method is successfully introduced to coat titanium implants with osteointegrative coatings [7–10, 12–17]. Important advantages of these ceramic like oxide layers are a special porous structure, a high adherence in the range of up to 26 MPa at the basic implant, the possibility to modify the chemical coating composition and the long term stability of these oxide films. The coatings are composed of compounds containing elements from both the electrolyte as well as from the anode material. Elements such as Ca or P can be incorporated into the surface oxide through selected electrolyte and coating conditions. So the presence of Ca can influence the cell growth and bone attachment on implant surfaces advantageous [18]. It may be anticipated that other elements for instance the trace element selenium as a

coating constituent also affects the biocompatibility of such coatings. Selenium is essential for mammals and it has been found in all tissues at different concentrations. Based on inorganic Se sources selenoproteins e.g. selenocysteine act from antioxidant defense to multible aspects of mammalian metabolism [19, 20].

In the present study Se-incorporated anodic conversion oxide coatings are prepared by anodic spark deposition on titanium surfaces in Se-containing electrolyte systems. The surface morphology and the microstructure of these anodic oxide films are characterized by surface and solid state techniques such as scanning electron microscopy, electron probe microanalysis and Raman spectroscopy. Based on these observations, a possible constitution of the oxide film is proposed. Results of cell culture experiments are discussed to compare the biocompatibility of the Se-incorporated anodic conversion oxide coatings with natural titanium oxide films at commercial pure titanium.

Materials and methods

ASD coating and surface characterization

The coatings were prepared in an electrochemical cell by the anodic spark deposition technique using a DC Delta Elektronika BV power supply SM 300-5 assisted by a Hameg function generator HM 8131-2 for the pulse generation. A titanium foil (Aldrich) of 0.127 mm thickness and 99.7% purity was used as the anode while platinum wire constituted the cathode. For the cell culture investigations Ti cylinders of 0.5 mm thickness and 5 mm diameter were used.

Aqueous solutions of 0.13 m $Ca(H_2PO_4)_2$ and Na_2SeO_4 (p.a. Fluka) as Se source were applied as electrolytes. The Se concentrations varied from 0.33% to 1.5% and a composite of 0.02 m $Ca(H_2PO_4)_2$, 0.13 m Na_2SeO_4 and 0.25 m H_3PO_4 was used to coat the Ti samples for the cell tests. The solutions were in a 250 mL double-wall glass beaker continuously magnetically stirred. The electrolyte temperature of 30 °C was thermostatically controlled. All titanium samples were chemically polished for 10 s in a mixture of phosphorus, hydrofluoric and nitric acid (H_3PO_4/HF/HNO_3) in a ratio of 49/24/27 vol. %, and ultrasonically cleaned in water followed by 2-propanol rinsing. At first an anodic pre spark film with 80 mA/cm^2 was potentiodynamically formed until sparking occurred. The ASD current density was up to 0.6 A/cm^2. After the coating process, the specimens were rinsed in distilled water and 2-propanol, dried and stored in air.

For characterization, specimens were examined in planar and in cross sectional view by a JEOL JSM 840 A SEM. Raman spectroscopy was performed on a DILOR XY with an optical multi-channel analyzer, the 514.5 nm line of an argon laser with 30 mW power was utilized. Electron probe microanalysis (EPMA) to determine the concentration of the chemical elements was carried out on a Cameca SX100.

Cell culture tests

The cell culture test was performed by using a human enoral osteoblast cell culture model. Proliferation of bone cells and the expression of TGF-beta were examined. TGF-beta (Transforming Growth Factor-beta—TGF-β) is a noncollagen bone protein which plays an important role in mineralization [21, 22].

After approval through the Ethics Committee of the University of Leipzig, education and written agreement of the contributor, human maxillary bone samples without any clinical or radiographic evidence of pathology were obtained undergoing dental surgery at the Department of Oral-, Maxillo- and Plastic Facial Surgery, University of Leipzig. The samples were immediately placed in sterile 0.05 M phosphate-buffered saline, and cultured.

By means of a Neubauer chamber (Feinoptik Bad Blankenburg) 4,000 cells/sample were seeded and incubated in an atmosphere of 5% CO_2 + 95% air at 37 °C for the experimental time of 3, 5, 7 or 10 days on Lab Tec^{TM} II Chamber Slide^{TM}-System. The cell culture medium (Osteoblastenmedium; Fa. PromoCell; Heidelberg) was completely changed every 3 day. Towards reaching required time, cell cultures were fixed and incubated with the primary antibody against bone growing proteins like Bone Sialoprotein (BSP), TGF-beta and others.

For the immunohistochemical detection of TGF-β the secondary antibody goat-anti-mouse-Cy3 (Jackson Immuno Research) was added accordingly. Terminal cell nuclei were tinged with DAPI (4′,6-Diamidino-2-phenylindol) as a standard marker binding to DNA and fluorescensing at 461 nm (Serva).

Six successive sections each sample were photographed twice with the digital camera Axiocam (Zeiss) installed on the fluorescence microscope Axioplan (Zeiss) at 200× magnification. The first, photographed with DAPI-filter, was employed to count the DAPI-labeled cells on the surface of the samples. The second, photographed with TRITC-filter, provided a basis to aquire quantitative volume of TGF-β expressed by the enoral human Osteoblasts on the material surface. The quantitative volume was determined over a standardised measurement and counting via optical density mean analysis, (gray value divided by exposure time) using the photo program Axio Vision (Zeiss).

Results and discussion

Coating preparation and characterization

In the selected aqueous electrolyte systems, under anodic polarization, titanium generates a passivating titania (TiO_2) film which can be modified by further increase of anodic potential. When the anodic potential exceeds the characteristic value required for a passivating electrolytic system, then solid state reactions initiated by spark discharges occur. ASD takes place during the dielectric breakdown of the insulating oxide film at the surface of the anode and is accompanied by visible plasma like micro sparking at the anode surface [1–6].

The resulting conversion coating is composed of compounds containing elements from both the anode metal and the electrolyte constituents [4, 14].

Figure 1 shows the characteristic initial breakdown voltage versus the Se concentration of different electrolytes. A subsequent increase in Se concentration leads to a logarithmic drop of the initial breakdown voltage. This drop is not only explainable by a simultaneous raising of the electrolytic conductivity. But it also indicates the influence of the dissociated selenate ion of the ASD coating conversion mechanism during its incorporation. In contrast to thermically or in the pre spark region generated titanium oxide films the conversion coatings fabricated by ASD show a micro structuring of the surface. Due to the plasma like state of the surface and the resulting short time fused oxides, the anodically erupted gases oxygen and steam can form a characteristic surface structure of clearly visible oxide meltings and a porous and spongy interconnected micro structure. Figure 2 shows a characteristic surface morphology of a DC generated porous conversion coating with caterpillar related structures of molten oxides.

The influence of DC and AC pulse current on the surface morphology is shown in the Figs. 2–5. The DC generated anodic spark plasma leads to a rough, porous and heterogeneously structured topography, whereas dielectric breakdown by pulse current generates more well fused surface oxide structures (Figs. 4, 5). These different morphologies are explainable by the resulting different energy densities during the anodic plasma reactions. DC leads to a higher local point current density and a corresponding higher anodic gas evolution that cumbers the build up of homogeneous surface oxide topographies. The micropores of the coatings were up to 4 μm in diameter and the microprojections were up to 6 μm in height (Fig. 6).

A SEM micrograph of a cross section shows that the coatings consist of two vertical distinguishable segments. Immediately on the titanium metal anode surface a pore free barrier layer of up to 1 μm thickness (I) of amorphous TiO_x [6] is found. Across this barrier layer the anodic potential drops drastically and the corresponding electric field strength E rises about 10^6 V/m, providing the required high potential for the anodic spark and plasma discharges. In contact with this barrier layer is a second coating segment designated by a porous structure with up to 8 μm thickness (II). Structure and chemical composition of its outermost layer are decisive for the biological coating properties.

The quantitative composition of the coatings and the concentration of the incorporated Se were investigated by electron probe microanalysis. Figure 7 shows the Se amount in the coating as a function of the applied anodic cell voltage.

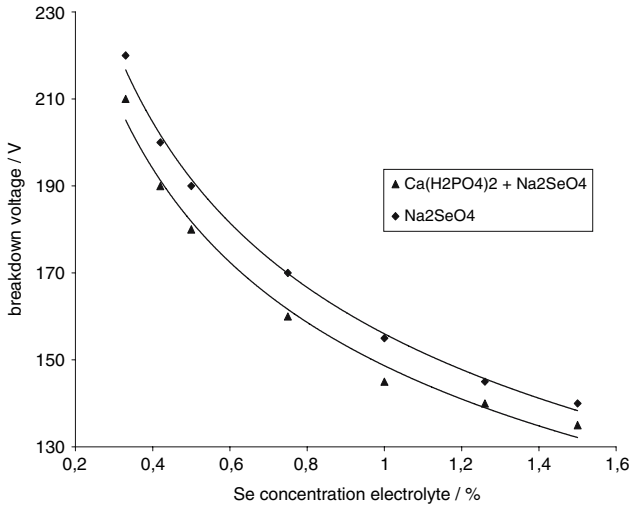

Fig. 1 Characteristic initial breakdown voltage versus the Se concentration for sodium selenate and the 0.13 m $Ca(H_2PO_4)_2$/Na_2SeO_4 electrolyte system

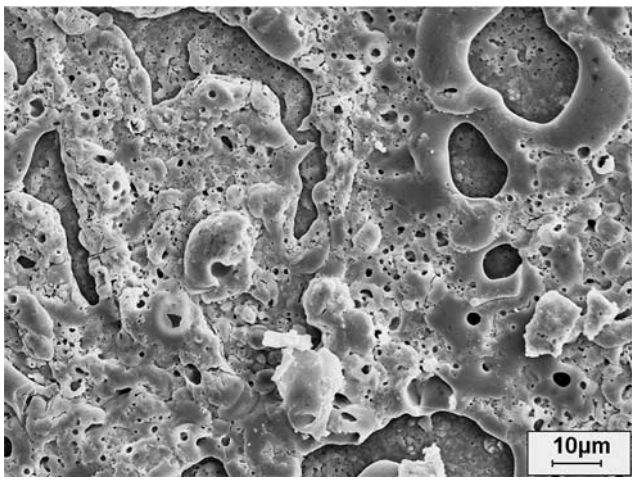

Fig. 2 DC generated conversion coating with molten oxide structures, sodium selenate elektrolyte (170 V; 0.75% Se)

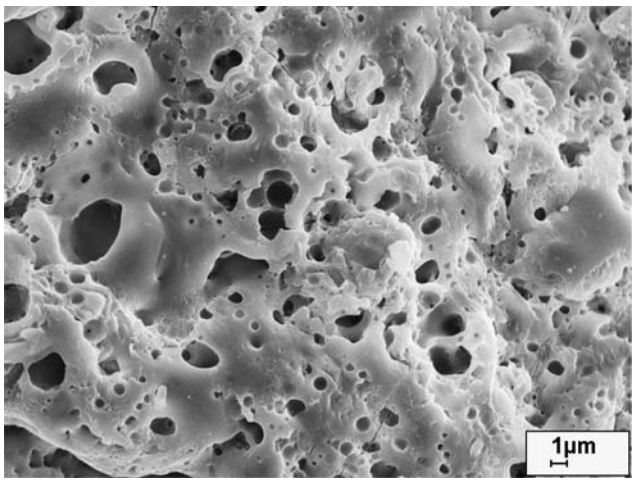

Fig. 3 Porous surface structure of a DC generated ASD coating (150 V), electrolyte 0.13 m $Ca(H_2PO_4)_2$ + 1% Se

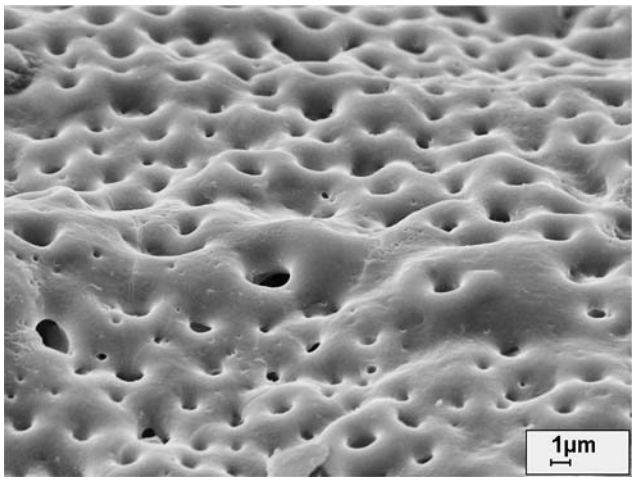

Fig. 4 SEM picture of a pulse current generated ASD coating (110 V) with undulated surface topography, electrolyte 0.13 m $Ca(H_2PO_4)_2$ + 1% Se, (SEM 65° tilt)

A detectable Se incorporation starts at about 60 V and increases up to the commencement of the anodic plasma reactions. During the plasma assisted conversion layer growth the Se concentration of the coating remains nearly constant. It shows that the Se incorporation for the ASD coatings is limited, investigations with Se electrolyte concentrations of 0.5% and 1.5% also confirm this result in principle. This behaviour is caused by the nature of the generated glass ceramic like oxide coatings consisting of solid solutions and its limited solubility in the solid state oxide systems $TiO_2/CaO/P_2O_5/SeO_2$ and TiO_2/SeO_2, respectively. Associated $[TiO_6]$ octahedrons and $[PO_4]$ tetrahedrons of different degrees of condensation may act as network former [14, 23]. Because of their higher ion radius of 99 pm calcium ions occur in the glass matrix as a

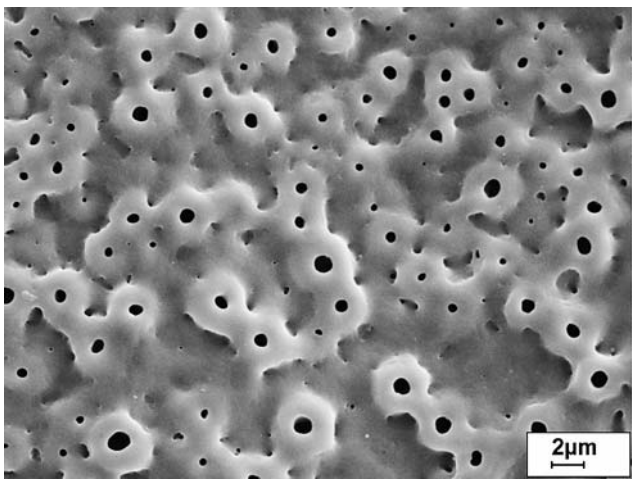

Fig. 5 Fused glass ceramic like oxide structures of a pulse current generated ASD coating (110 V), electrolyte 0.02 m $Ca(H_2PO_4)_2$, 0.13 m Na_2SeO_4 and 0.25 m H_3PO_4

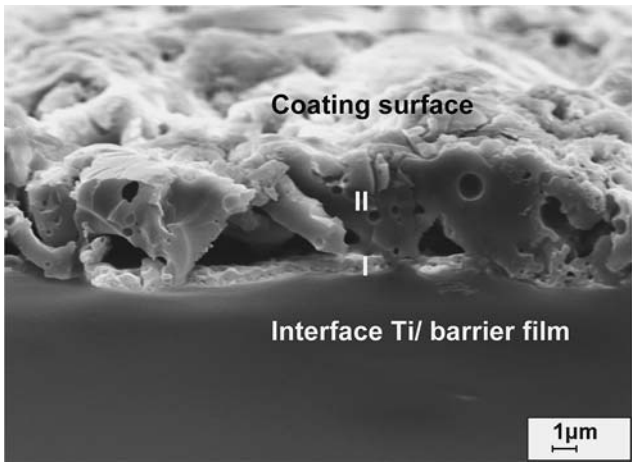

Fig. 6 SEM micrograph of a cross section of DC generated ASD coating, electrolyte 0.13 m $Ca(H_2PO_4)_2$ + 1% Se

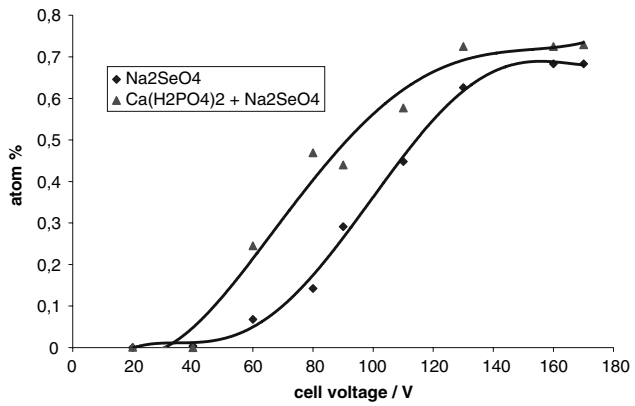

Fig. 7 Se concentration in DC generated ASD coatings, electrolytes 0.13 m $Ca(H_2PO_4)_2$ + 0.75% Se and sodium selenate electrolyte (0.75% Se)

modifier. It is assumed that the films contain Se as coordination polyhedrons of [SeO_4] and sodium ions which are randomly distributed inside the coating network [23]. The average composition of coatings generated in 0.13 m $Ca(H_2PO_4)_2$ + 1% Se by DC and pulse current consists of 9–13% Ti, 68–74% O, 3–6% Ca, 9–12% P and up to 1% Se and traces of 0.3% Na.

X-ray measurements show the amorphous, glassy like nature of the investigated coatings. Raman spectroscopy, which is known to be more sensitive to shorter-range order of some amorphous materials, including TiO_2 films [24, 25], has been performed to complement the analytical results and to detect possible nano crystalline phases of the coating constituents. Films generated in $Ca(H_2PO_4)_2$ solutions exhibit the nanophase anatase structure as a modification of titania, verified by observation of Raman vibration modes at 145 cm^{-1} (E_g, not shown), 394 cm^{-1} ($B1_g$), 512 cm^{-1} ($A1_g$) and 630 cm^{-1} (E_g) [26] as seen in Fig. 8. The broad Raman bands and the underlying continuum indicate the small crystalinity and the amorphous character of these coatings. A drastic modification of the film structure was observed when selenium was added to this electrolyte or the coatings were generated in pure sodium selenate electrolytes. In these cases no nano crystalline phases of titanium oxides or other chemical compounds were detected because the incorporated Se influences the plasma chemical ASD reactions and the phase composition and coating structure as a constituent of this amorphous oxide system.

In vitro cell investigations

During the in vitro cell proliferation test with osteoblasts on different surfaces the following results were observed. The blue (DAPI)-coloured nuclei of the cells were counted after 3, 5, 7 and 10 days (Fig. 9). At the same time the expression of TGF-beta has been measured (Fig. 10).

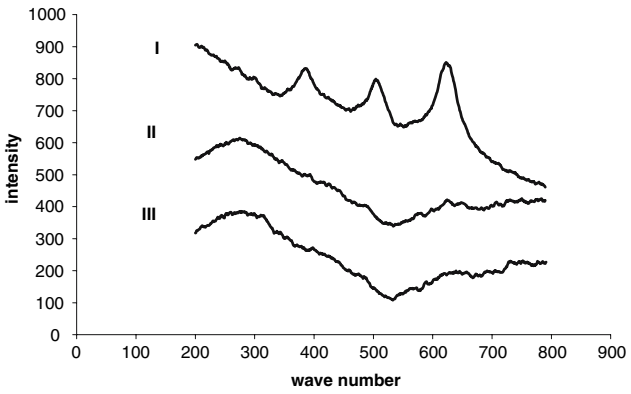

Fig. 8 Raman spectra of DC generated ASD coatings (0.2 A/cm^2), electrolytes 0.13 m $Ca(H_2PO_4)_2$ (I), $Ca(H_2PO_4)_2$ + 0.75% Se (II), and pure sodium selenate electrolyte (0.75% Se, III)

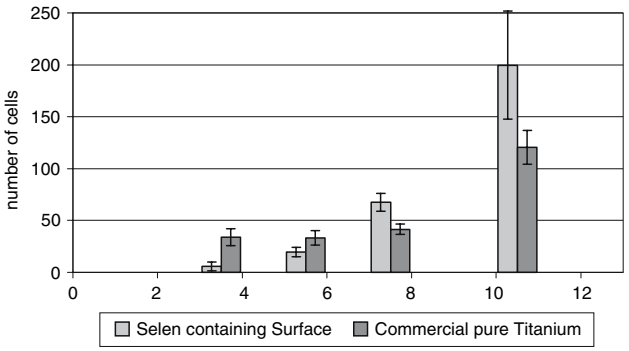

Fig. 9 Number of cells on different surfaces over time in a human bone cell culture system from enoral bone

The expression of TGF-beta in cells on the surface of selenium modificated implants increased in tendency more than on CPT implants. Only to the 3 day less TGF-beta is observed on the selenium surface. A statistical difference has been found at the 5 and 10 day. At the 7 and 10 day also the number of cells was significantly higher on the Se-modificated implants than on the CPT implants. This reflects that the proliferation of enoral bone cells differentiation starts a little bit later, but than much more faster. The differentiation (measured as expression of TGF-beta) shows a similar behaviour but with a 3 days earlier start. Recent studies show that TGF-beta significantly enhances the proliferation of cells and the mineralization on implant materials [21, 22].

Conclusions

The following structural model for the description of anodic Se incorporated oxide films is proposed. The results of the surface- and solid state analytical investigations show that amorphous glassy like coatings on the titanium have been formed in all cases of the described experimental conditions. Films generated in $Ca(H_2PO_4)_2$ solutions exhibit the nanophase anatase structure as a modification of titania. The coatings are spongy and porous in the outermost surface region, with pore diameters up to 4 µm. At the interface metal/oxide a barrier film up to 1 µm thickness is responsible for the high electric field strength E of about 10^6 V/m required for the ASD process. In accordance with the found chemical composition and the ratio of the coating forming elements, the structure can be described as a system of glass like solidified oxides.

Associated [TiO_6] octahedrons and [PO_4] tetrahedrons of different degrees of condensation may act as network former [4, 14]. Because of their higher ion radius of 99 pm

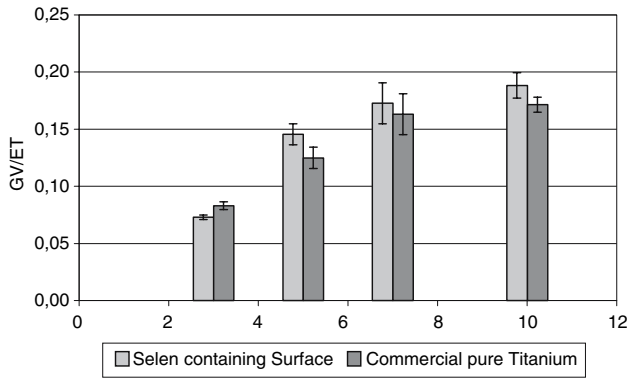

Fig. 10 Expression of TGF-Beta on selenium containing surface (left) and commercial pure titanium (right) over time (GV/ET: Gray value/exposure time; see materials and methods)

calcium ions occur in the glass matrix as modifier. Within the coating the generation of nano crystalline aggregations and cluster formations of the oxide system $xCaO{\cdot}yP_2O_5{\cdot}zTiO_2$ are possible. It is assumed that the films also contain coordination polyhedrons of $[SeO_4]$ and sodium ions which are randomly distributed inside the coating network. Further investigations are needed to verify this structure model.

First results of testing bone cell reaction to selenium containing anodic oxide surfaces in a cell culture system from human are encouraging.

Acknowledgements The support of this work by ZL Microdent Attachment, Breckerfeld and Heraeus Kulzer, Hanau, Germany is gratefully acknowledged.

References

1. L. L. GRUSS and W. MCNEIL, *Electrochem. Technol.* **1** (1963) 283
2. P. KURZE, W. KRYSMANN, J. SCHRECKENBACH, T. SCHWARZ and K. RABENDING, *Cryst. Res. Technol.* **22** (1987) 53
3. J. P. SCHRECKENBACH and K. RABENDING, *J. Chem. Edu.* **8** (1996) 782
4. G. P. WIRTZ, S. D. BROWN and W. M. KRIVEN, *Mater. Manuf. Process.* **6** (1991) 87
5. A. L. YEROKHIN, X. NIE, A. LEYLAND, A. MATTHEWS and S. J. DOWEY, *Surf. Coat. Techn.* **122** (1999) 73
6. J. P. SCHRECKENBACH, F. SCHLOTTIG, G. MARX, W. M. KRIVEN, O. O. POPOOLA, M. H. JILAVI and S. D. BROWN, *J. Mater. Res.* **4** (1999) 1437
7. V. M. FRAUCHIGER, F. SCHLOTTIG, B. GRASSER and M. TEXTOR, *Biomaterials* **25** (2004) 593
8. H. ISHIZAWA and M. OGINO, *J. Biomed. Mat. Res.* **29** (1995) 65
9. J. HALL and J. LAUSMAA, *Appl. Osseointegr. Res.* **1** (2000) 5
10. P. KURZE, W. KRYSMANN and W. KNÖFLER, *Stomatol. DDR* **36** (1986) 549
11. H. GUO and M. AN, *Thin Solid Films* **500** (2006) 186
12. W. KNÖFLER and P. KURZE, *Zahn Mund Kieferhk* **74** (1986) 706
13. H.-L. GRAF, B. GEU, W. KNÖFLER and A. HEMPRICH, *Z Zahnärztl Implantol* **18** (2002) 169
14. J. P. SCHRECKENBACH, F. SCHLOTTIG, M. TEXTOR, G. MARX and N. SPENCER, *J. Mater. Sci. Mater. Med.* **10** (1999) 453
15. H.-J. OH, J. LEE, Y. JEONG, Y. KIM and C.-S. CHI, *Surf. Coatings Technol.* **198** (2005) 247
16. H.-L. GRAF, W. KNÖFLER and A. HEMPRICH, *Implantologie* **12** (2004) 257
17. X. ZHU, J. CHEN, L. SCHNEIDER, R. REICHEL and J. GEISGERSDORFER, *Biomaterials* **25** (2004) 4087
18. S. H. MAXIAN, J. P. ZAWADSKY and M. G. DUNN, *J. Biomed. Mater. Res.* **28** (1994) 1311
19. J. KÖHRLE, R. BRIGELIUS-FLOHE, A. BÖCK, R. GÄRTNER, O. MEYER and L. FLOHE, *Biol. Chem.* **381** (2000) 849
20. L. SCHOMBURG, U. SCHWEIZER and J. KÖRLE, *CMLS Cell. Mol. Life Sci.* **61** (2004) 1988
21. X . NIE, W. TIAN, Y. ZHANG, X. CHEN, R. DONG, M. JIANG, F. CHEN and Y. JIN, *Cell Biol. Int.* **30** (2006) 295
22. H. ZHANG, M. S. ARONOW and G. A. GRONOWICZ, *J. Biomed. Mater. Re. A* **75** (2005) 98
23. W. VOGEL, *Chemistry of Glass* (Springer, 1992)
24. M. OCANA, J. GARCIA-RAMOS and C. SERNA, *J. Am. Ceram. Soc.* **75** (1992) 2010
25. J. P. SCHRECKENBACH, N. MEYER, G. MARX, B. T. LEE and W. M. KRIVEN, *Appl. Surf. Sci.* **205** (2003) 97
26. H. K. VARMA, P. K. PILLAI, T. V. MANI, K. G. K. WARRIER and A. D. DAMONDARAN, *J. Am. Ceram. Soc.*, **77** (1994) 129